Fractal Analysis for Natural Hazards

Edited by
G. Cello and B. D. Malamud

Geological Society
Special Publication 261

Crustal stress and seismic activity in the Ionian archipelago as inferred by satellite- and ground-based observations, Kefallinìa, Greece

MAURIZIO POSCOLIERI[1], EVANGELOS LAGIOS[2], GIOVANNI P. GREGORI[1], GABRIELE PAPARO[1], VASSILIS A. SAKKAS[2], ISSAAK PARCHARIDIS[5], IGINIO MARSON[3], KONSTANTINOS SOUKIS[4], EMMANUEL VASSILAKIS[4], FRANCESCO ANGELUCCI[1] & SPYRIDOULA VASSILOPOULOU[2]

[1]*Istituto di Acustica O. M. Corbino (CNR), via Fosso del Cavaliere 100, 00133 Roma, Italy (e-mail: giovanni.gregori@idac.rm.cnr.it; gabriele.paparo@idac.rm.cnr.it; maurizio.poscolieri@idac.rm.cnr.it; pangelu@tiscalinet.it)*

[2]*National and Kapodistrian University of Athens, Geophysics Laboratory, Space Applications in Geosciences, Panepistimiopolis, Ilissia, Athens 157 84, Greece (e-mail: sakkas@geol.uoa.gr; lagios@geol.uoa.gr; Vassilopoulou@geol.uoa.gr)*

[3]*Dipartimento di Ingegneria Navale, del Mare e per l'Ambiente, Università di Trieste, via Valerio 10, 34127 Trieste, Italy; Istituto Nazionale di Oceanografia e Geofisica Sperimentale (OGS), Borgo Grotta Gigante 42/c, 34010 Sgonico, Trieste, Italy (e-mail: marson@univ.trieste.it; marson@ogs.trieste.it)*

[4]*Department of Geology, University of Athens, Athens, Greece (e-mail: evasilak@geol.uoa.gr; soukis@geol.uoa.gr)*

[5]*Harokopio University of Athens, Athens, Greece (e-mail: parchar@hua.gr)*

Abstract: Different observational techniques are compared in order to investigate possible correlations in seismic activity. The study site is the island of Kefallinìa (Greece), where measurements available included (1) DInSAR, DGPS, and DEM data, (2) soil exhalation measured by monitoring Radon (Rn) well content, and (3) acoustic emissions (AE) at high and low frequency (point-like records with high temporal resolution). AE records provide: (1) relative time variation of the applied stress intensity and (2) the state of fatigue of stressed rock volumes, the AE source. Our results indicate that the large spatial scale (poor time resolution) may be considered quite satisfactory, whereas fractal analysis of the AE time series displayed some discrepancies when compared to analogous investigations in the Italian Peninsula. Therefore, some refinement is needed in order to reach more precise interpretations of the relevant information available with this kind of data. However, both sets of observations appear in agreement with each other, although more exhaustive investigations would require a suitable array of point-like AE and Rn (or other) measuring sites, as well as longer data series. The latter are particulary helpful for detailed interpretations of the different occurrences within tectonically complex settings where crustal stress crises are marked by various types of geological phenomena.

Slow deformations and crustal stress propagation characterize geodynamic phenomena over regional space scales much larger than the areas struck by a seismic event. The entire scenario can be depicted in terms of a perturbation propagating through the crust and giving rise to local deformations, and eventually triggering an earthquake wherever a sufficient amount of potential elastic energy has been stored by the system. We attempt to discuss the observational evidence eventually supporting such interpretation, based on observations carried out in the island of Kefallinìa (Cephalonia) in Western Greece.

Different observational techniques are considered. The first is measurement of acoustic emission (AE) in the ultrasound range: high-frequency or HF AE at 160 or 200 kHz and low-frequency or LF AE at 25 kHz. These are very effective for monitoring phenomena that occur on a submicroscopic scale and precede extreme events by

From: CELLO, G. & MALAMUD, B. D. (eds) 2006. *Fractal Analysis for Natural Hazards.* Geological Society, London, Special Publications, **261**, 63–78.
0305-8719/06/$15.00

several months. The temporal resolution of AE is very high, and the information is point-like, and premonitory phenomena deal with an area as large as $\sim 10^6$ km^2. A few other techniques are much more effective in terms of spatial coverage over a given area, although the temporal resolution is unavoidably very low. For instance, Differential Interferometric Synthetic Aperture Radar (DInSAR) and Differential Global Position System (DGPS) are the best known standard satellite-based techniques for crustal deformation measurements. Topography is another information source, which is utilized by means of suitable Digital Elevation Model (DEM) database.

The aims of the present study are (1) to show that DInSAR and DGPS are capable of measuring some important aspects of pre- and post-seismic crustal deformation; (2) to demonstrate the synergistic integration, and complementary use of two satellite-based techniques, with the AE technique and soil exhalation; and (3) to investigate by means of a suitable analysis of a DEM some complementary geomorphologic information related to the tectonic setting of the island.

Tectonic setting

The Hellenic arc-trench system (Fig. 1a) is a tectonically very active area formed 80 Ma BP (millions of years before present) as an oceanic subduction zone. Eventually the area became a case history of interaction between two continental (African and Eurasian) masses. Kefallinìa is one of the Ionian Islands in western Greece and it is located on the NW sector of this narrow zone of convergence. The Ionian basin is still being subducted to the south, under the Aegean domain, whereas, to the north, continental collision occurred between the Apulia microplate and the Hellenic foreland (Sachpazi *et al*. 2000). Those two domains are linked by a major right–lateral NE–SW trending transform fault (*KF*), located offshore, west of the island (Fig. 1b; Louvari *et al.* 1999; Sachpazi *et al*. 2000).

Kefallinìa is built up mainly by alpine Mesozoic–Cenozoic sedimentary rocks belonging to the external units of the Hellenides (Fig. 2a). During the Neogene, they were part of the Hellenide fold-and-thrust belt. On top of them, mainly in the south-southwestern sector of the island, younger Plio-Quaternary sediments lay uncomformably (Underhill 1989). The deformation of the Alpine stage is recorded mainly by NW–SE trending thrusts. These older structures are crosscut by more recent NE–SW trending faults, which in some cases exhibit a significant right–lateral movement.

Four major tectonic blocks can be distinguished on the island, based on lithology, on similar structural features, and on a common evolution during the upper Quaternary: (1) the *Erissos* peninsula block (northern part of the island); (2) the *Paliki* peninsula block (western part of the island); (3) the *Ainos* block (central and eastern part of the island); and (4) the *Argostoli* block (southwestern part of the island). Each of these major blocks consists of several subordinate units and is flanked by a major thrust fault. Most subordinate units have more or less distinct geological features, on account of their difference in geological evolution during some stage. However, during the Late Quaternary, some of them were unified and compressed into the four major blocks of the island (see Fig. 2b).

Several strong earthquakes ($M > 6.0$) have occurred in the Kefallinìa area. The last great event ($Mw = 6.7$) occurred on 17 January 1983, if we do not consider the 14 August 2003 earthquake ($Mw = 6.2$), involving mostly Lefkada island, northeast of Kefallinìa (Papadopoulos *et al.* 2003; Pavlides *et al.* 2004). Since then, no other event of comparable magnitude has occurred in the area, although a great number of smaller events ($4.0 < Mw < 5.0$) have been observed, and at least one event of $Mw \approx 5.0$ is expected every year. The island is considered a *Very High Seismic Risk Zone* and is the subject of several investigations. We note that there is a substantial difference between the tectonic setting of Kefallinìa and that of the Italian peninsula; hence, it is difficult to compare these two geodynamic scenarios.

GPS techniques

The DGPS observations were taken from 23 GPS stations (Fig. 3) spread over the island, which are 'linked' and referenced to GPS stations on continental Greece. These were used to indicate possible tectonic deformation in Kefallinìa, with respect to the 'stable' mainland. The GPS network was installed in October 2001 and their relative measurements were carried out in January and September 2003. The station locations (average spacing ~ 10 km) were selected according to the main geological structural units and to seismic activity concentration. The aim was to study the tectonic deformation triggered by faulting and by pre- and post-seismic activity.

A station in the central part of Kefallinìa (at Mt Ainos) was chosen as a reference (with fixed coordinates). In addition, the network was referenced to the Dionysos (DION) permanent GPS station in the Athens area, about 290 km east of Kefallinìa, for monitoring larger-scale regional movements.

Six geodetic receivers of WILD type (SR299 and SR399) were used for the GPS measurements. The Static Kinematic Software (SKI Pro, Version 3.2

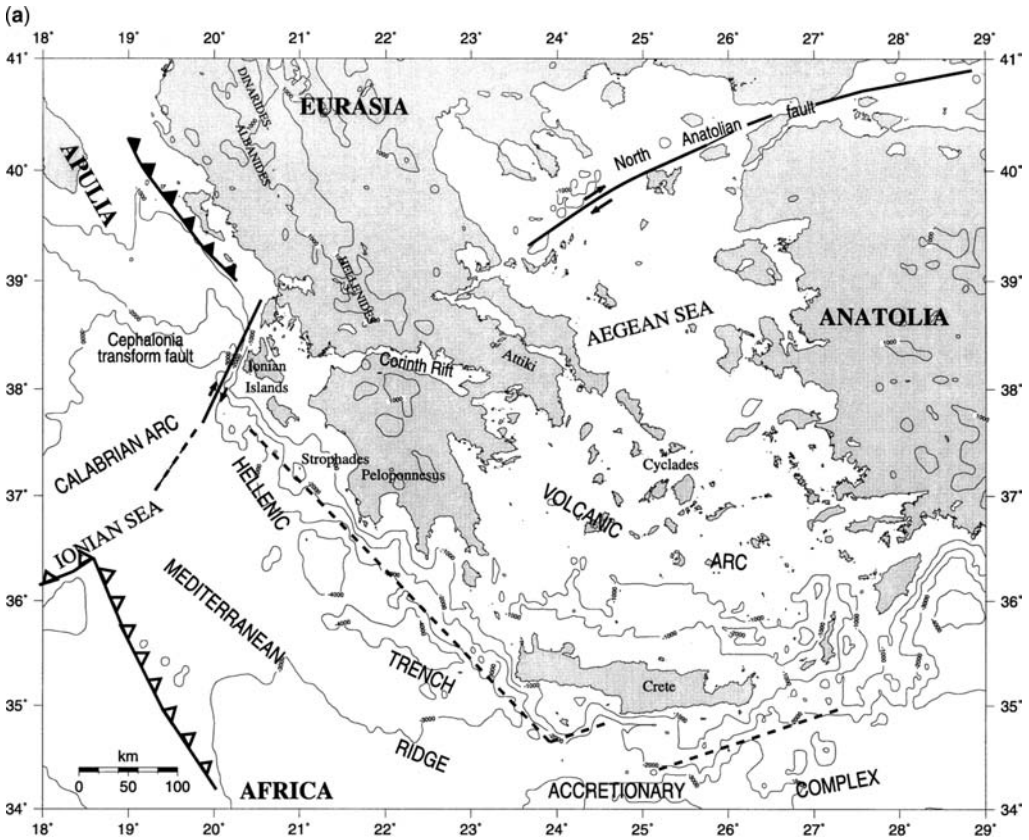

Fig. 1. (**a**) Sketch map of Europe–Africa plate interaction in the region of the Hellenic subduction. Active volcanic arc in the Aegean sea. Frontal thrusts indicated: the line with full triangles for the collision with Eurasia of Apulia, the submerged northern continental margin of the Ionian sea being part of Africa; the line with open triangles for the front of the accretionary complexes, in the west for the Calabrian one, in the east for the Hellenic one and the Mediterranean Ridge. In this subduction zone, the Hellenic Trenches, between full and dashed lines, are interpreted as outer arc basins made of upper plate material of the Aegean extensional region as well as a continental backstop to the accretionary complex. Major active strike–slip faults are the North Anatolian fault, along which Anatolia is extruded, and the Cephalonia Transform Fault, the subject of the present study, which links collision with the western Hellenic subduction. After Sachpazi *et al*. (2000).

1999) of Leica allowed *in situ* processing and adjustment of the GPS measurements. Post-processing of the GPS data was performed using the Bernese GPS Software Version 4.2 (Hugentobler *et al.* 2001), together with post-computed satellite orbits (downloaded from the International GPS Service, IGS). In this way, the error estimate of the coordinates of the stations on Kefallinìa could be improved. Such adjusted values for the different periods of observations were considered, and an accuracy of 2–3 mm in the horizontal and 4–6 mm in the vertical component was finally achieved.

The horizontal vector of deformation in the Kefallinìa network, when referenced to DION, has a NNE direction with an amplitude of ∼20 mm, which is consistent with a clockwise rotation and with the regional tectonics of western Greece (Cocard *et al.* 1999). Concerning the DION station, an annual motion in a SSW direction of ∼12 mm could be accurately defined. The final result is suggestive of a clockwise rotation of western Greece (Cocard *et al.* 1999) (Fig. 4).

The local deformation was with reference to the Mt Ainos network. After the first remeasurement (January 2003), a small deformation of 4–10 mm was found in the horizontal component, and the vertical deformation range was 10–20 mm. The vector of the horizontal ground motion indicated a clockwise rotation around the main tectonic block of Mt Ainos, with small local discrepancies. The vertical

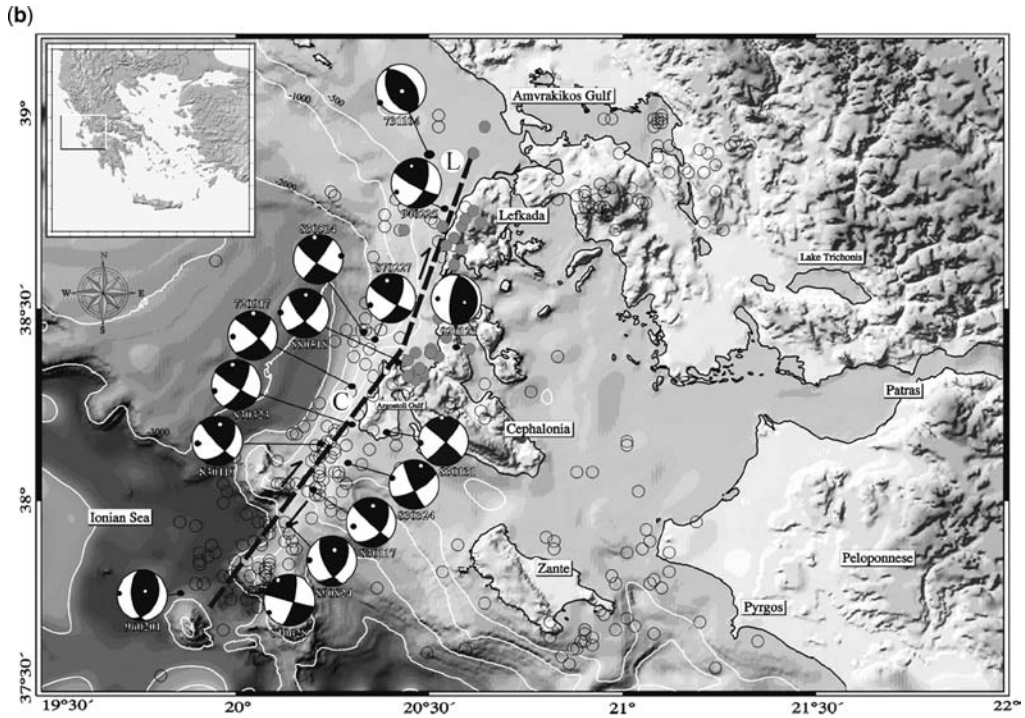

Fig. 1. (**b**) The Kefallinìa Transform Fault. The Kefallinìa segment of the fault is marked as C and the Lefkada segment as L. The distribution of well-located seismicity (open circles) and epicentres of microearthquakes (filled circles), as well as the focal mechanisms of strong events are also shown. Figure and captions after Louvari *et al.* (1999).

movement show a general uplift of the island, with areas of subsidence to be associated with step-like faulting in the southwestern slopes of Mt Ainos and along the southern coast of the island.

The DGPS results of the September 2003 remeasurement were strongly affected by the major 14 August 2003 earthquake (Fig. 1c) that occurred on the island of Lefkada (Papadopoulos *et al.* 2003; Pavlides *et al.* 2004). Aftershocks appeared linearly concentrated along the northern part of Kefallinìa. Stations located on this side of the island showed strong ground southeast motions, while the area was subsiding. Stations located further south appeared less affected, maintaining the same pattern as that inferred from the first remeasurement.

DInSAR techniques

DInSAR has already proved its capability of providing images of ground surface deformation (Gabriel *et al.* 1989; Zebker *et al.* 1994; Massonnet & Feigl 1995, 1998; Peltzer & Rosen 1995; Hanssen 2001; Salvi *et al.* 2004; Wright *et al.* 2004). The technique was used to plot interferograms, covering the investigated area, using radar images of the ESA satellites *ERS-2* and *ENVISAT*. Differential interferometric images covering the period 28 September 1995 to 14 August 1998 seem to coincide with the ground deformation observed in the island, although the period is not exactly the same. The DInSAR image reveals deformations (Fig. 5) located in the northern part of Kefallinìa, and mainly in the eastern sector, hence confirming the ground activity observed by DGPS measurements through time.

A pair of SAR images was selected with a small baseline ($B_p = 12$ m) although with long time separation (*ERS-1*, 28 September 1995; and *ERS-2*, 14 August 1998). Ground deformation could thus be observed over a long period of time, during which no seismic event occurred. In general, the results of this analysis are consistent with the ground deformation recorded on the island by means of DGPS techniques. In more detail, every 360° fringe circle represents one predefined great difference Δz (called altitude of ambiguity) for every fringe of the interferogram. It can be

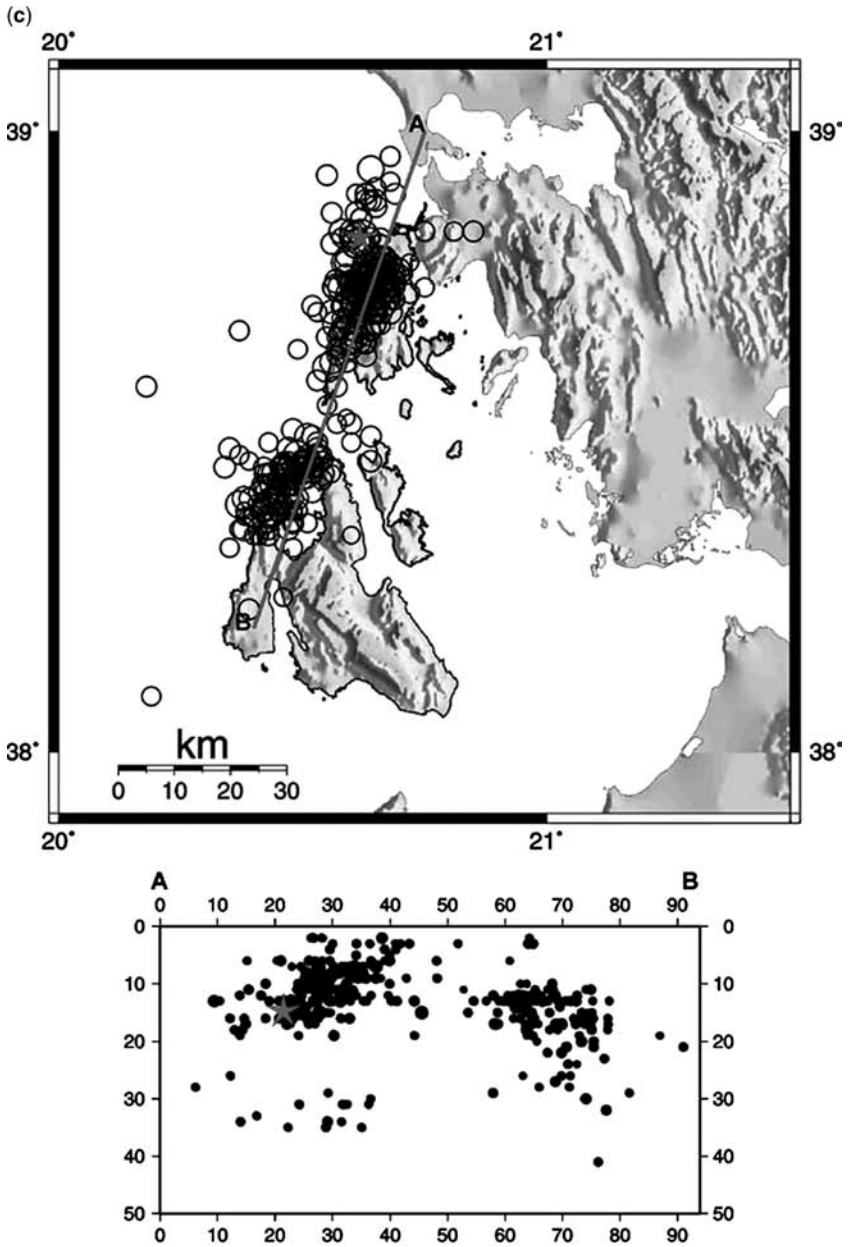

Fig. 1. (**c**) The Lefkada earthquake, 14 August 2003, Mw = 6.2. Two clusters operated simultaneously. The first Mw = 4 event unambiguously located in the southern cluster occurred 9 min after the main shock. After Zahradník *et al.* (2005).

calculated as a function of the wavelength of the radar signal, of the altitude of the satellite, of the angle of the signal, and of the perpendicular distance (B_{perp}) between the two orbits. In the present application, Δz is ~495 m. Therefore, every fringe represents ~495 m in height.

Coherence characterizes the quality of the interferogram. In the present application, the coherence for the larger part of the island was quite low, leaving only selected areas with good coherence. The long temporal separation and the dense vegetation that covers most of the island are mainly

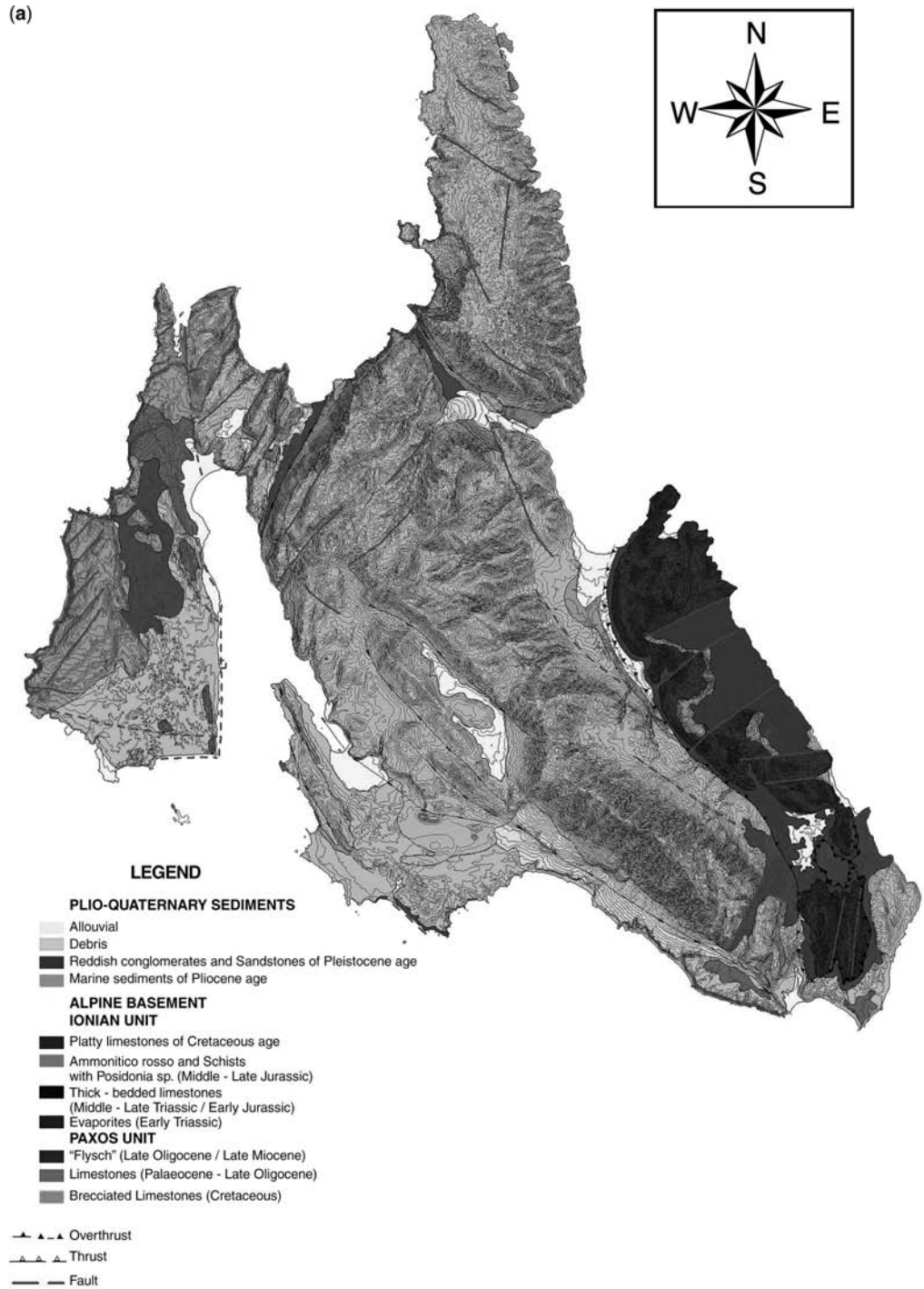

Fig. 2. (**a**) Geological map of Kefallinìa.

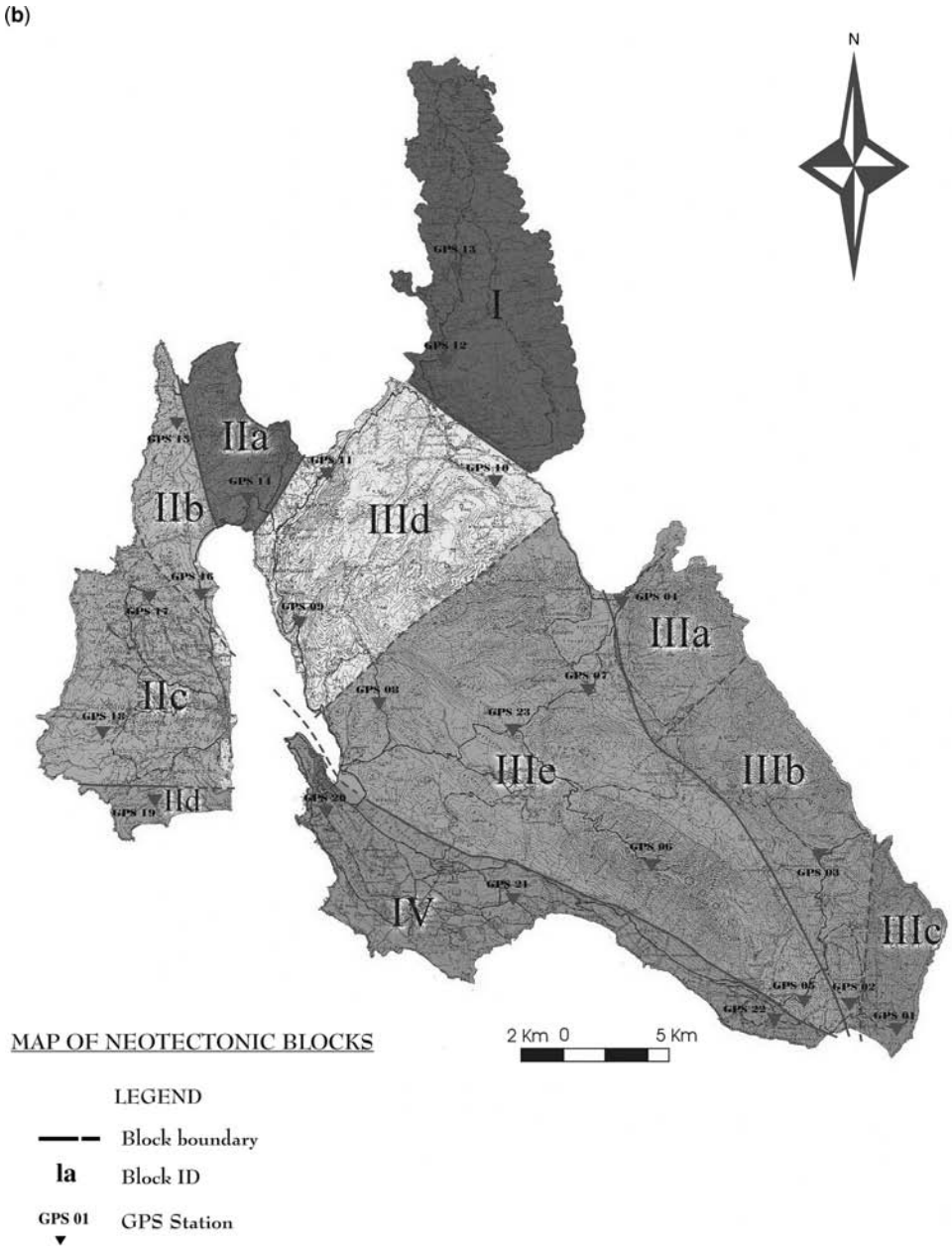

Fig. 2. (**b**) Map of structural blocks of Kefallinìa.

responsible for such poor coherence. In the Lixouri peninsula, in the west of the island, the vegetation is not dense. However, the poor coherence resulted from the geological features, characterized by loose formations and strong erosion.

The areas of good coherence are limited to the NE and SE of the island. We can define three areas:

(1) *Northeastern area*. One fringe equals 28 mm of deformation along the line of sight and the one

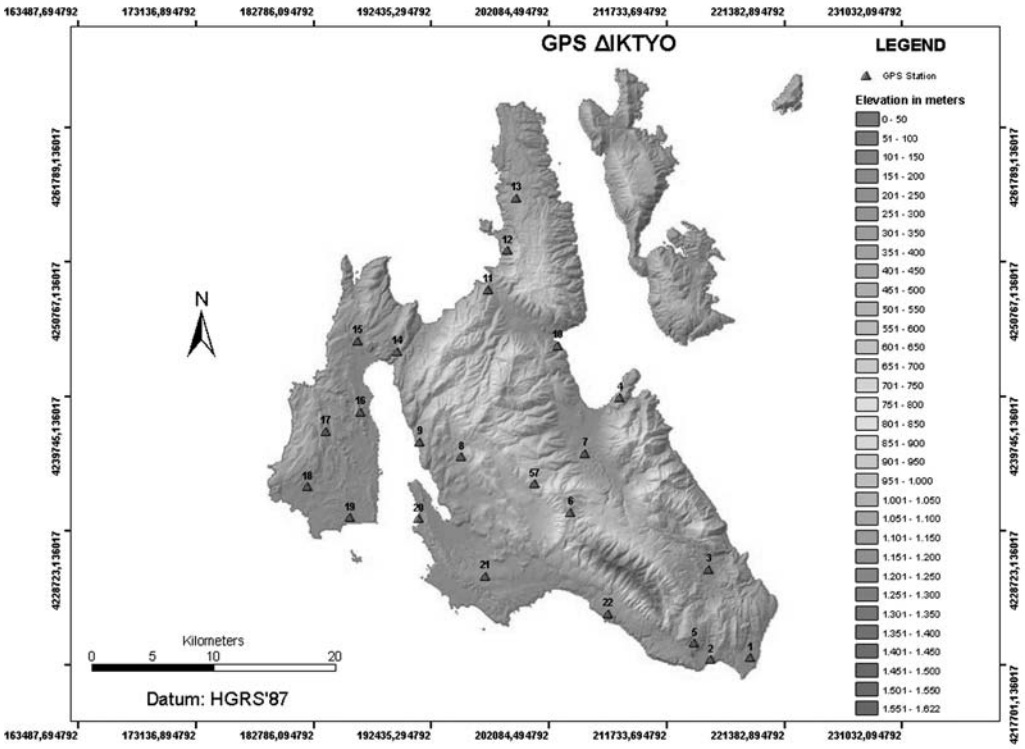

Fig. 3. Location of the 23 GPS stations operating on the island.

fringe is formed along the topography of the area. The height difference in the area that covers the deformation fringe is about 500 m and is almost equal to Δz. This evidence, combined with the tectonic characteristics of the area and the control of the GPS results, denotes that the fringe represents the topography of the area rather than ground deformation.

(2) *Agia Efimia area*. In this area, a small, roughly circular, fringe can be defined. The spatial coverage of this fringe does not coincide with the topography and is located in an area where a NNW–SSE faulting zone occurs. It is not easy to explain this feature in detail, mainly because of its limited extension. However, the ground deformation associated with this fault zone could be related to localized phenomena and/or to vertical subsidence, which occurs in this area, according to GPS data.

(3) *Digaleto area*. In this area we observe the most interesting fringes. The coherence is good and almost two fringes of ground deformation are found, although the height difference in the area is only $\sim$350 m. In the *Digaleto* area the outcropping geological units are made of Cretaceous carbonate rocks of *Ammonitico rosso* formation, schists of Middle–Upper Jurassic times, Evaporites and Breccias of the Lower Triassic. The zone of deformation is also limited by two E–W and NE–SW oriented faults.

DEM techniques

The geomorphic characteristics of the island can be quantitatively defined by a landform classification procedure, based on the analysis of the local morphological setting (Parcharidis *et al.* 2001; Cavalli *et al.* 2003; Parmegiani & Poscolieri 2003; Adediran *et al.* 2004). Geomorphometric data were gathered by processing a raster DEM (20 m per pixel ground resolution) produced by digitizing contour lines of a 1:50,000 scale map. The method is based on the application of multivariate statistics to an eight-layer stack, which describes the topographic gradients, measured along the eight azimuth orientations of the neighbourhood of every DEM pixel. This approach permits a quick estimate of the spatial distribution of different types of slope steepness, and a discrimination of areas characterized by similar local geomorphologic settings. Hence, it is possible to focus on changes in shape,

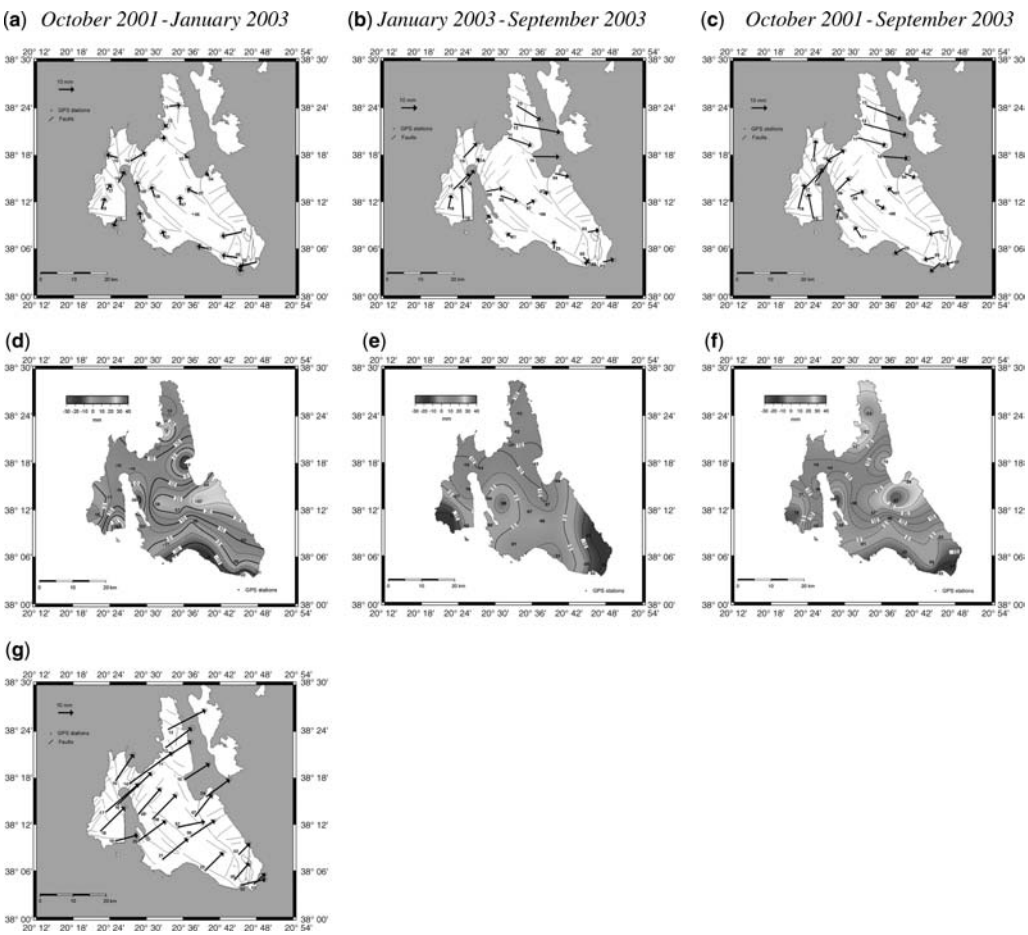

Fig. 4. DGPS measurements. Comparison between first and second determinations (plots in the first column), second and third (second column), and first and third (third column), respectively. The first row deals with horizontal displacements, and the second row with vertical motions. The third row shows the regional large-scale displacement compared to the mainland (DION station).

orientation and steepness, and to stress the impact of erosional and tectonic processes on the overall relief. The classification technique chosen for processing gradient values was an unsupervised cluster analysis technique, ISODATA (Tou & Gonzales 1974; Hall & Khanna 1977). The following input parameters were chosen for the application of this multivariate procedure: 15 classes, threshold percent change of 1.0%, and 25 maximum iterations.

The resulting classification map (Fig. 6) assigns every class a given grey shade. Classes were later statistically analysed by computing mean and standard deviation of the eight layers, which represent the elevation differences of every DEM pixel with respect to the neighbourhood. In addition, after calculating *slope* and *aspect* values from the same DEM, the mean and variance of these parameters and of height were computed for all 15 ISODATA classes, and compared with the aforementioned eight-layer statistics, in order to give a correct geomorphic interpretation of the classification (Fig. 7). The preliminary analysis and interpretation of the geomorphometric image (Fig. 6), compared with the geological and tectonic block map (Fig. 2b), show a good correspondence with the geostructural setting of the area.

AE techniques and soil exhalation

Since 1 February 2003, a multifrequency AE station has been in operation in Kefallinìa, at a very central

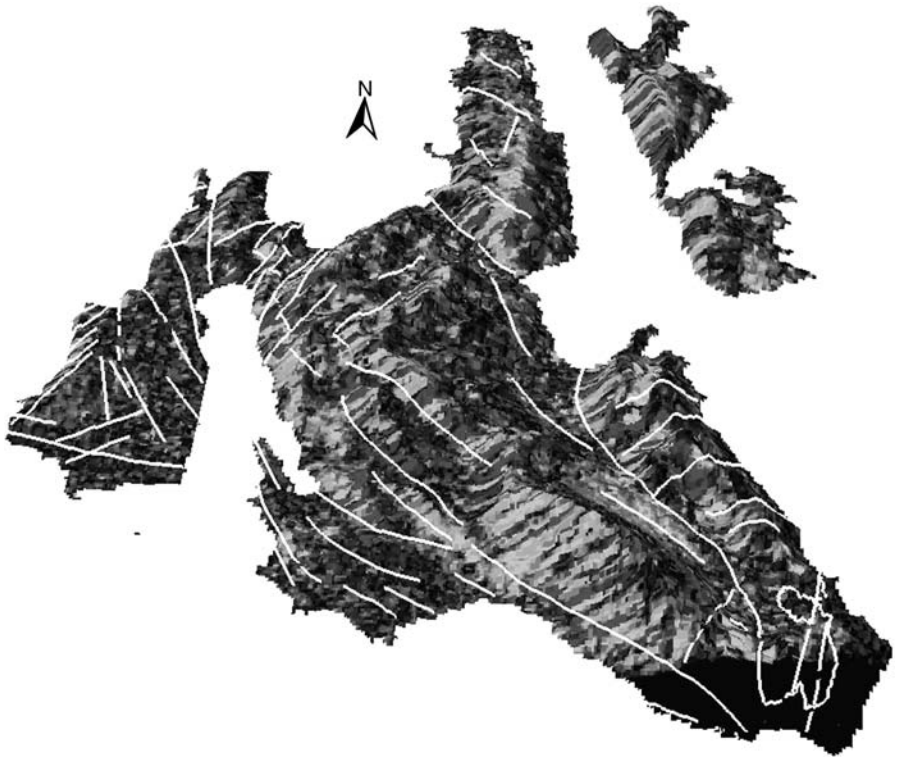

Fig. 5. Three-dimensional representation of the *interferogram* obtained by processing a couple of *ERS-1* and -2 SAR images covering Kefallinia, with the main fault system of the island superimposed.

location of the island, and a nearby well is being monitored for Radon (Rn) content. Every AE datum is a 30 s integrated signal at its respective frequency. Periods of anomalous AE activity were observed. Consistent with previous evidence from the Italian peninsula (Paparo *et al.* 2006, this volume), they denote microdeformations preceding a seismic crisis. The HF AE (at 200 kHz) are correlated with Rn exhalation from the well.

The rationale of the analysis is hereafter briefly explained. The AE signal is released whenever some atomic bonds yield within a crystal structure, and it propagates through the entire solid probe within which the crystals are embedded. Because of this, our AE recorder should be located on top of a rocky outcrop, which is the terminal of a huge natural probe of unknown extension underground. Whenever a tectonic event makes the orientation of the natural probe change, the conspicuous crustal stress that is thus generated causes some AE release. The intensity of the AE recorded signal depends on the (unknown) efficiency of the waveguide that transfers the AE signal from its source through the detector. The HF AE will be the first observed, corresponding to the yield of some lesser and tiny pores of the solid body. As soon as such pores coalesce into comparatively larger pores, some progressively lower frequency AE will be observed. These AE of progressively lower frequency will be later followed by mechanical vibrations of still lower frequency, until the seismic roar is heard, the vibration of mechanical structures occurs, and finally the seismic shock occurs. An earthquake, however, is not just a catastrophe that causes damages whenever some mechanical vibrations happen. It is, rather, a complex crustal phenomenon that must be investigated in all its aspects, beginning from its atomic level that releases some HF AE until the occurrence of the 'catastrophe'.

In addition to the AE signal *per se*, which reveals the occurrence of some change in the statics and tectonics of the area, implying a time variation of the crustal stress, fractal analysis of the time series of the AE signals (see Appendix, page 59, for details) gives an effective indication of the state of *fatigue* of the solid rocks that are releasing the AE. (Note, 'When the resultant of all the forces

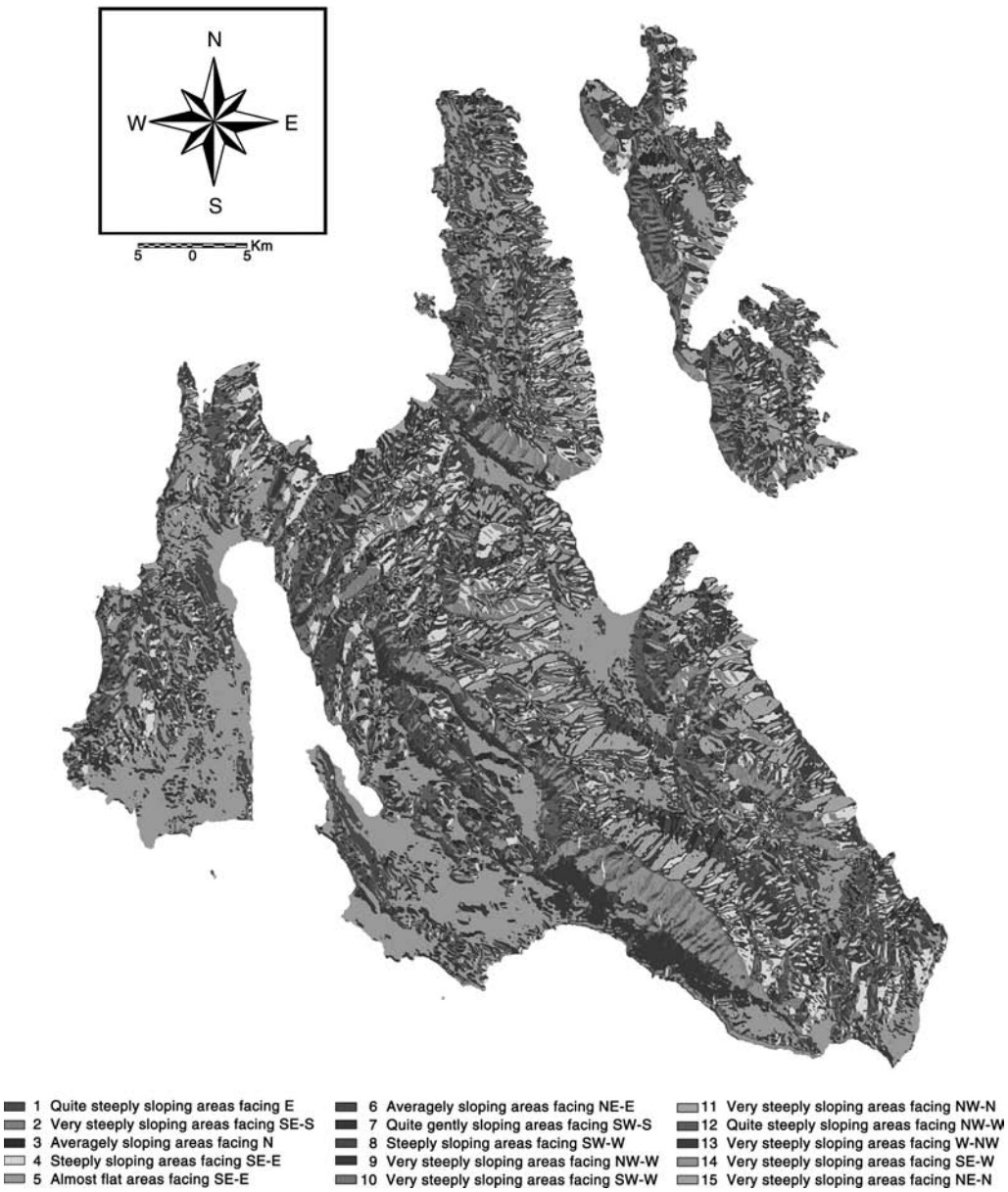

Fig. 6. Geomorphometric map of the Kefallinìa island. For explanation see Figure 7.

in a body is zero the body is said to be in equilibrium. This will be the case if it is at rest or moving with constant speed in a straight line. Both of these cases are grouped under the common heading of problems in statics' (Sears 1950, p. 15). Consider some huge rock, and it changes its orientation with respect to the local gravity vector. The internal stress distribution shall change accordingly, eventually causing a release of AE.) In fact, the intensity of the AE release depends (although not linearly) on the intensity of the applied stress. In contrast, the response of a material is different depending on its ageing, which depends on its fatigue. Such property is revealed by the type of time sequence of the observed AE signals. However, it is impossible to

ISODATA MORPHO-UNITS	GEOMORPHOMETRIC UNITS INTERPRETATION	ELEVATION DIFFERENCES (m)			ELEVATION (mean, std values)	SLOPE (mean, std values)	ASPECT (mean, std values)
1 (759 pixels) 0.04%	Quite steeply sloping areas facing W	+1.69	-1.42	-8.01			
		+3.10		-7.06	257.2 m	14.6°	264.4°
		+3.15	-0.35	-7.48	(231.9 m)	(4.3°)	(14.0°)
2 (93036 pixels) 4.78%	Very steeply sloping areas facing SE-S	-11.63	-8.43	-5.01			
		-3.21		+3.32	465.3 m	24.5°	158.8°
		+5.23	+8.43	+11.62	(282.9 m)	(6.3°)	(13.7°)
3 (129102 pixels) 6.63%	Averagely sloping areas facing N	+5.31	+4.67	+4.03			
		+0.72		-0.65	403.3 m	13.9°	222.7°
		-3.92	-4.69	-5.32	(290.0 m)	(4.2°)	(157.4°)
4 (146216 pixels) 7.50%	Steeply sloping areas facing SE-E	-10.47	-3.20	+4.13			
		-7.29		+7.29	424.6 m	21.9°	114.3°
		-3.96	+3.26	+10.42	(288.9 m)	(6.4°)	(13.5°)
5 (467171 pixels) 23.98%	Almost flat areas facing SE-E	-0.37	-0.12	+0.13			
		-0.25		+0.25	201.0 m	4.3	174.4°
		-0.14	+0.11	+0.35	(219.5 m)	(2.3°)	(99.1°)
6 (238753 pixels) 12.25%	Averagely sloping areas facing NE-E	-1.89	+2.02	+5.88			
		-3.94		+3.92	354.7 m	13.2°	63.6°
		-5.95	-2.02	+1.91	(279.3 m)	(3.8°)	(21.4°)
7 (223322 pixels) 11.46%	Quite gently sloping areas facing SW-S	-1.85	-3.69	-4.62			
		+1.39		-1.37	285.0 m	11.1°	203.9°
		+4.59	+3.24	+1.88	(231.6 m)	(3.5°)	(27.5°)
8 (97052 pixels) 4.98%	Steeply sloping areas facing SW-W	+2.79	-3.79	-10.35			
		+6.56		-6.56	399.2 m	21.1°	239.8°
		+10.34	+3.86	-2.65	(267.8 m)	(3.9°)	(12.9°)
9 (57891 pixels) 2.97%	Very steeply sloping areas facing NW-W	+15.49	+4.03	-7.47			
		+11.60		-11.54	428.7 m	31.5°	288.8°
		86	-3.93	-15.41	(264.4 m)	(5.4°)	(11.6°)
10 (40777 pixels) 2.09%	Very steeply sloping areas facing SW-W	+7.95	-4.48	-16.77			
		+12.37		-12.33	512.6 m	33.5°	250.0°
		+16.85	+4.60	-7.65	(371.2 m)	(4.8°)	(11.7°)
11 (67085 pixels) 3.44%	Very steeply sloping areas facing NW-N	+15.02	+10.2	+5.32			
		+4.98		-4.88	507.1 m	29.8°	333.8°
		-5.12	-10.2	-14.98	(327.7 m)	(5.3°)	(13.9°)
12 (128858 pixels) 6.61%	Quite sleeply sloping areas facing NW-W	+7.10	+1.76	-3.59			
		+5.42		-5.39	360.5 m	16.3°	286.9°
		+3.75	-1.69	-7.09	(262.8 m)	(4.6°)	(16.4°)
13 (85317 pixels) 4.38%	Very steeply sloping areas facing NE-E	-5.84	+3.74	+13.32			
		-9.69		+9.69	481.2 m	27.7°	69.0°
		-13.31	-3.64	+6.04	(332.5 m)	(5.0°)	(12.9°)
14 (81816 pixels) 4.20%	Very steeply sloping areas facing SW-S	-4.86	-9.81	-14.58			
		+4.88		-4.78	575.7 m	28.9°	206.1°
		+14.58	+9.81	+5.03	(343.3 m)	(5.2°)	(12.0°)
15 (91209 pixels) 4.68%	Very steeply sloping areas facing N-NE	+5.16	+9.37	+13.57			
		-4.19		+4.29	492.5 m	27.5°	33.3°
		-13.55	+9.36	-4.97	(334.7 m)	(5.4°)	(52.5°)

Fig. 7. Height/slope/aspect mean values and morphostructural interpretation of the elevation differences between every pixel and the eight neighbours, for the 15 classes recognized in this study.

detect very feeble AE signals. It is reasonable to guess that the kind of temporal sequence associated with a given state of fatigue remains invariant starting from the undetectable and very feeble AE signals through their more intense and recordable AE impulses. Therefore, we have to transform the original AE record into a sequence of impulses – that is, in the language of the mathematician, in order to recognize the fatigue of the medium, we have to consider a point-like process. (See Appendix, page 59, for details.) This was also shown by investigating several laboratory specimens of different kinds (investigations not reported here). As far as the geophysical applications are concerned, a great advantage was obtained from the possibility of comparing AE records collected from different geological settings, dealing either with crustal stress originated by some external (tectonic) cause (such as typically occurs in the case of earthquakes), or by some endogenous source (such as occurs in geothermal or volcanic areas).

Figure 8 shows the results for the Kefallinìa island. The AE records plotted are the smoothed weighted running average over ± 12 hours. (Note,

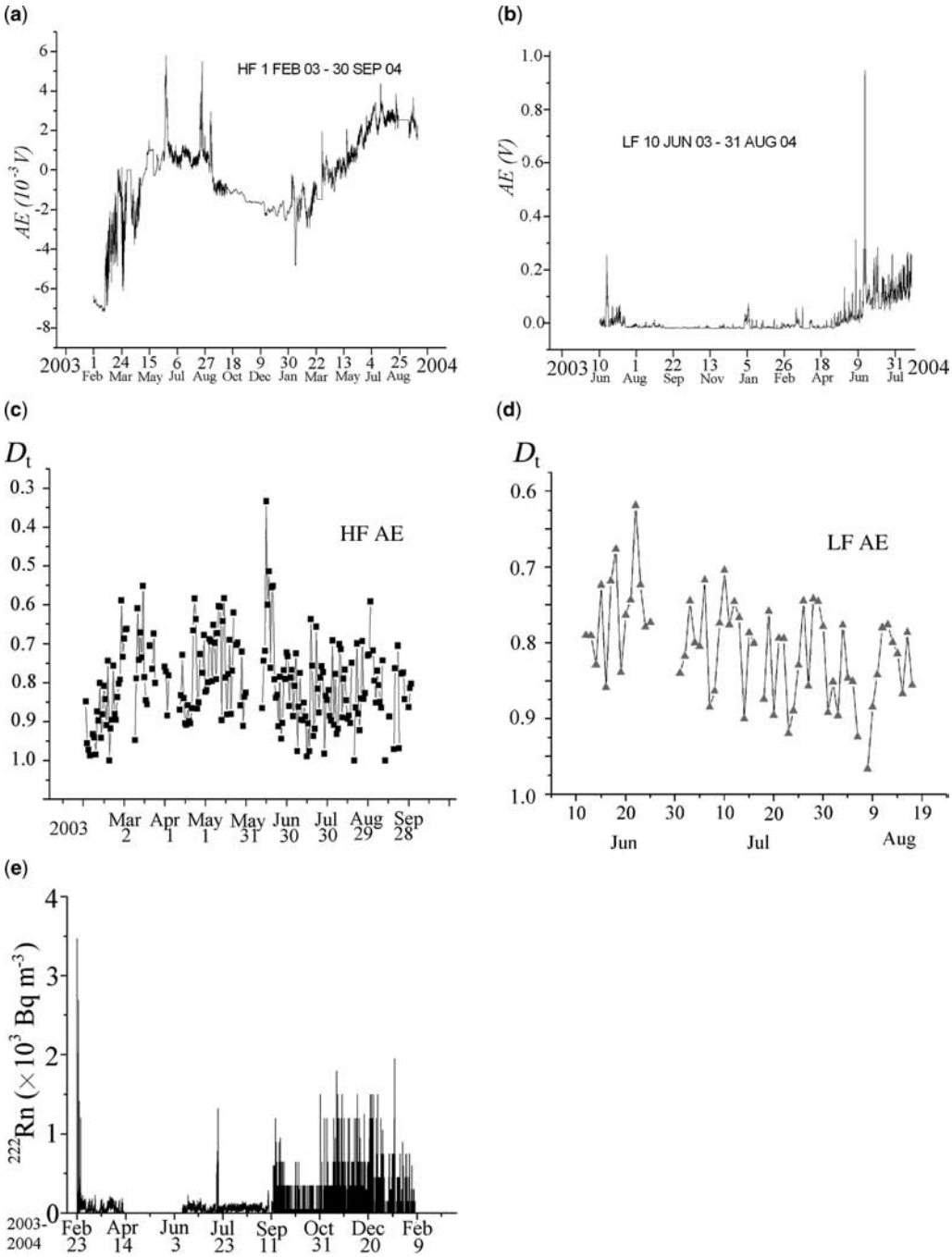

Fig. 8. (**a**) through (**e**) top to bottom, left to right: HF AE (left column), LF AE (right column), and Rn exhalation (bottom). The second row shows the fractal dimension D_t v. date, dealing with a reduced time interval (more extended analysis in progress). Please, note that large HF AE are correlated with rapid Rn flux increase. (Bq indicates Becquerel, unit for radioactivity; for comments see text.)

we carried out a running average over a total time lag of 24 hours, by applying a triangular filter, with maximum weigh at the centre of the time interval, and weigh linearly decreasing to zero from the entry time instant t, to $t - 12$ hours and to $t + 12$ hours, respectively.) Compared with previous case histories from the Italian Peninsula (see Paparo *et al.* 2006, this volume), a remarkable feature is the large scatter of the fractal dimension D_t v. time for both HF and LF AE (Fig. 8c, d). The LF AE series is more limited in time, because of the failure of the system as a result of a flood. The steep increase of HF AE in February 2003 seems to correlate with the large Rn maximum (Fig. 8a, e). The HF AE peak in the middle of June 2003 (Fig. 8a) ends when the peak of LF AE starts (Fig. 8b), and both peaks are followed by a Rn peak observed at the end of July 2003 (Fig. 8e).

The HF AE (Fig. 8a) displays some activity. The fluctuations reveal that the AE sensor was unable to recover during the time lag elapsing between every two subsequent AE signals. That is, the sensor experienced a very rapid sequence of AE signals. This supports the fact that the entire region was presumably subject to some relevant stress propagation during the entire time interval. The HF AE spikes denote, presumably, some local features associated with the yield of microstructures at a site comparatively close to the AE recording site. Another possibility is that the AE source was at a comparatively great distance, but the AE source was much more intense. This second possibility could be suggestive of a correlation between AE and the Lefkada earthquake (Fig. 1c), and the subsequent peaks could be better explained according to the first mechanism. In more detail, the system after the Lefkada earthquake remained perturbed during the entire period in which aftershocks were observed, and it shifted to an apparently quiet trend when the aftershocks ceased. Then, according to the HF AE, the system remained in a comparatively quiet state for a while, until January 2004, when it started to be perturbed anew by some activity shown by a scattered and increasing trend.

The LF AE plot in Figure 8b shows some activity during June–July 2003, preceding the Lefkada earthquake by approximately two months. According to the same rationale, some lesser activity in January to March 2004 could be associated with four events of Mw $\sim$ 4 with an epicentre in northern Kefallinìa. Shortly after this occurrence, an increasing trend occurred after 18 April 2004, showing that the region had very frequent AE signals, and the sensor could not recover between any two subsequent signals. Independent of their specific physical interpretation (which, in any case, appears still fairly premature), three different observations can be made from the LF AE plot in Figure 8b. First, there is essentially no trend except during the very last period of records, when it increases. Second, a simple scatter of points is superposed, almost like noise (however, is not noise) and this should have a physical implication. Third, the scatter or 'noise' seems to increase significantly, being in some way approximately correlated with the amplitude of the increasing trend. During May 2004 a remarkable amount of seismic activity was concentrated in the northern region of Zàkinthos.

The large LF AE peak observed shortly after 9 June 2004 (Fig. 8b) could be an object of serious concern. This much larger peak could denote that either the AE source is much closer to the AE sensor than in 2003, or that a new earthquake is forthcoming, at a comparatively great distance, but of some stronger intensity. Obviously, this is not a prediction. One could tentatively consider this feature as being one possible precursor, suitably correlated with other evidence by means of other techniques.

On the other hand, such a phenomenon could be interpreted differently. The HF AE trend (Fig. 8a) can be considered as separating the long-range from the short-range trend. The short-range HF AE trend displays some apparently erratic variations, which, as mentioned above, ought to reflect local stress and microdeformation, although displaying the aforementioned correlation with aftershocks. The long-range HF AE trend clearly displays a possible yearly variation, which is not significant *per se*, because, strictly speaking, several years of records ought to be available. However, the same yearly trend, although eventually phase shifted, is observed also in the Italian Peninsula. If this inference is confirmed, an interpretation has to be attempted. Considering the conspicuous difference in tectonic settings between Italy and Kefallinìa, a tentative possible guess is that a yearly wave of crustal stress is steadily involving the entire central and western Mediterranean area, potentially associated with astronomical forcing. For the time being this is mere speculation, and a correct interpretation can be given only by considering HF AE records collected at several different locations, perhaps operated non-simultaneously, in order to map the apparent yearly trend, and its amplitude and relative phase. With this perspective of the HF AE, the LF AE appears comparatively less interesting, as no apparent or suspected yearly trend is observed.

In general, however, the AE records seem to provide a significant and unprecedented monitoring of the evolution of the crust during its preparatory stage before the eventual occurrence of an earthquake. It appears to be a useful technique also for *diagnosing* the temporal evolution of crustal stresses, independently of whether an earthquake is going to occur or not.

Conclusions

With respect to the AE technique, Kefallinìa and the Italian peninsula, although having very different tectonic settings, display some interesting analogies, although every realistic inference on crustal stress evolution requires arrays of simultaneously operated AE recording stations. More in general, this would allow us to better explore the potential of fractal analysis of AE time series signals in order to furnish important information on the state of fatigue of stressed crustal rock volumes. Regarding the other techniques that are considered in the present study, their results appear to be in agreement with each other, although, as expected, no final conclusion seems as yet possible. The 'large-scale' information derived from satellite remote sensing or from DEM analysis lacks any adequate time resolution. In contrast, the field records (AE and soil exhalation) have a good time resolution, although they are point-like, and one needs an array of recording points to obtain information valuable for geophysical inference. Our results might show, however, that the crustal stress in Kefallinìa island propagates and interacts with (or, perhaps, it contributes to generating) the highly complicated faulting network responsible for the seismicity of the area. The degrees of freedom of the system are, however, too large, and no simple or intuitive model can yet be proposed from the presently available database.

References

ADEDIRAN, O. A., PARCHARIDIS, I., POSCOLIERI, M. & PAVLOPOULOS, K. 2004. Computer-assisted discrimination of morphological units on north-central Crete (Greece), by applying multivariate statistics to local relief gradients. *Geomorphology*, **58**, 357–370.

CAVALLI, R. M., FUSILLI, L., PASCUCCI, S., PIGNATTI, S. & POSCOLIERI, M. 2003. Relationships between morphological units and vegetation categories of Soratte Mount (Italy) as inferred by processing elevation and MIVIS hyperspectral data. *In*: BENES, T. (ed.) *Proceedings of 22nd EARSeL Symposium and General Assembly*, Prague (Cleck Rep.), 4–6 June 2002, Millpress, Rotterdam (Netherlands), 573–579.

COCARD, M., KABLE, H. G. *ET AL.* 1999. New constraints on the rapid crustal motion of the Aegean region: recent results inferred from GPS measurements (1993–1998) across the West Hellenic Arc, Greece. *Earth and Planetary Science Letters*, **172**, 39–47.

GABRIEL, A. K., GOLDSTEIN R. M. & ZEBKER, H. A. 1989. Mapping small elevation changes over large areas: Differential radar interferometry. *Journal of Geophysical Research*, **94(B7)**, 9183–9191.

HALL, D. J. & KHANNA, D. 1977. The ISODATA method of computation for relative perception of similarities and differences in complex and real data *In*: ENSLEIN, K., RALSTON, A. & WILF, H. S. (eds) *Statistical Methods for Digital Computers* 3, John Wiley Pub., New York, 340–373.

HANSSEN, R. F. 2001. *Radar Interferometry. Data Interpretation and Error Analysis*. Kluwer Academic Publishers, Dordrecht.

HUGENTOBLER, U., SCHAER, S. & FRIDEZ, P. 2001. *Bernese GPS Software Version 4.2 Documentation*. Astronomical Institute University of Bern, Switzerland.

LOUVARI, E., KIRATZI, A. A. & PAPAZACHOS, B. C. 1999. The Cephalonia transform fault and its extension to western Lefkada island (Greece). *Tectonophysics*, **308**, 223–236.

MASSONNET, D. & FEIGL, K. L. 1995. Discrimination of geophysical phenomena in satellite radar interferograms. *Geophysical Research Letters*, **22**, 1537–1540.

MASSONNET, D. & FEIGL, K. L. 1998. Radar interferometry and its application to changes in the Earth's surface. *Review of Geophysics*, **36**, 441–500.

PAPADOPOULOS, G. A., KARASTATHIS, V., GANAS, A., PAVLIDES, S., FOKAEFS, A. & ORFANOGIAUNAKI, K. 2003. The Lefkada, Ionian Sea (Greece), shock (Mw 6.2) of 14 August 2003: Evidence for the characteristic earthquake from seismicity and ground failures. *Earth Physics Letters*, **55**, 713–718.

PAPARO, G., GREGORI, G. P., POSCOLIERI, M., MARSON, I., ANGELUCCI, F. & GLORIOSO, G. 2006. Crustal stress crises and seismic activity in the Italian peninsula investigated by fractal analysis of acoustic emissions, soil exhalation and seismic data emission (AE), soil exhalation and seismic data. *In*: CELLO, G. & MALAMUD, B. D. (eds) *Fractal Analysis for Natural Hazards*. Geological Society, London, Special Publications, **261**, 47–61.

PARCHARIDIS, I., PAVLOPOULOS, A. & POSCOLIERI, M. 2001. Geomorphometric analysis of the Vulcano and Nysiros island: clues of the defintions of their volcanic landforms. *In*: GIOVANNELLI, F. (ed.) *Proceedings of the International Workshop "The Bridge between Big Bang and Biology"*, Stromboli (Messina, Italy), 13–17 September 1999. CNR, President Bureau, Special Volume, 310–320.

PARMEGIANI, N. & POSCOLIERI, M. 2003. Studio dell'impatto antropico sull'assetto morfologico di un'area archeologica. *In*: *Proceedings of the 7th ASITA National Conference "L'informazione territoriale e la dimensione tempo"*, Verona (Italy), 28–31 October 2003, **2**, 1569–1574.

PAVLIDES, S. B., PAPADOPOULOS, G. A., GANAS, A., PAPATHANASSIOU, G., KARASTATHIS, V., KERAMYDAS, D. & FOKAEFS, A. 2004. The 14 August 2003 Lefkada (Ionian Sea) earthquake. *In*: *Proceedings of the 5th International Symposium on Eastern Mediterranean Geology*, Thessaloniki, Greece, 14–20 April 2004, Paper T5-34, 1–4.

PELTZER, G. & ROSEN, P. 1995. Surface displacements of the 17 May 1993 Eureka Valley, California, earthquake observed by SAR interferometry. *Science*, **268**, 1333–1336.

SACHPAZI, M., HIRN, A. *ET AL.* 2000. Western Hellenic subduction and Cephalonia Transform: local earthquakes and plate transport and strain. *Tectonophysics*, **319**, 301–319.

SALVI, S., GANAS, A. *ET AL.* 2004. Monitoring long-term ground deformation by SAR Interferometry: examples from the Abruzzi, central Italy, and Thessaly, Greece. *In*: *Proceedings of 5th International Symposium on Eastern Mediterranean Geology*, Thessaloniki, Greece, 14–20 April 2004, Paper T7-17, 1–4.

SEARS, F. W. 1950. *Mechanics, Heat and Sound*. Addison-Wesley, Reading, MA.

TOU, J. T. & GONZALES, R. C. 1974. *Pattern Recognition Principles*. Addison-Wesley, Reading, MA.

UNDERHILL, J. R. 1989. Late Cenozoic deformation of the Hellenic foreland, Western Greece. *Geological Society of America Bulletin*, **101**, 613–634.

WRIGHT, J., PARSONS, B., ENGLAND, P. C. & FIELDING, E. J. 2004. InSAR observations of low slip rates on the major faults of western Tibet. *Science*, **305**, 236–239.

ZAHRADNÍK, J., SERPETSIDAKI, A., SOKOS, E. & TSELENTIS, G.-A. 2005. Iterative deconvolution of regional waveforms and a double-event interpretation of the 2003 Lefkada earthquake, Greece. *Bulletin of the Seismological Society of America*, **95**, 159–172.

ZEBKER, H. A., ROSEN, P. A., GOLDSTEIN, R. M., GABRIEL, A. K. & WERNER, C. L. 1994. On the derivation of coseismic displacement-fields using differential radar interferometry – the Landers earthquake. *Journal of Geophysical Research*, **99(B10)**, 19617–19634.